

Influence of solar wind energy flux on the interannual variability of ENSO in the subsequent year

Sheng-Ping HE, Hui-Jun WANG, Yong-Qi GAO, Fei LI, Hui LI & Chi WANG

To cite this article: Sheng-Ping HE, Hui-Jun WANG, Yong-Qi GAO, Fei LI, Hui LI & Chi WANG (2018): Influence of solar wind energy flux on the interannual variability of ENSO in the subsequent year, Atmospheric and Oceanic Science Letters, DOI: [10.1080/16742834.2018.1436367](https://doi.org/10.1080/16742834.2018.1436367)

To link to this article: <https://doi.org/10.1080/16742834.2018.1436367>



© 2018 The Author(s). Published by Informa UK Limited, trading as Taylor & Francis Group



Published online: 12 Feb 2018.



Submit your article to this journal [↗](#)



Article views: 20



View related articles [↗](#)



View Crossmark data [↗](#)

Influence of solar wind energy flux on the interannual variability of ENSO in the subsequent year

HE Sheng-Ping^a, WANG Hui-Jun^{b,c,d}, GAO Yong-Qi^{d,e}, LI Fei^f, LI Hui^g and WANG Chi^g

^aGeophysical Institute, University of Bergen, Bjerknes Center for Climate Research, Bergen, Norway; ^bKey Laboratory of Meteorological Disaster, Collaborative Innovation Center on Forecast and Evaluation of Meteorological Disasters, Nanjing University of Information Science and Technology, Nanjing, China; ^cClimate Change Research Center, Chinese Academy of Sciences, Beijing, China; ^dNansen-Zhu International Research Centre, Institute of Atmospheric Physics, Chinese Academy of Sciences, Beijing, China; ^eNansen Environmental and Remote Sensing Center, Bergen, Norway; ^fNorwegian Institute for Air Research, Kjeller, Norway; ^gState Key Laboratory of Space Weather, National Space Science Center, Chinese Academy of Sciences, Beijing, China

ABSTRACT

Previous studies have tended to adopt the quasi-decadal variability of the solar cycle (e.g. sunspot number (SSN) or solar radio flux at 10.7 cm (F10.7) to investigate the effect of solar activity on El Niño–Southern Oscillation (ENSO). As one of the major terrestrial energy sources, the effect of solar wind energy flux in Earth's magnetosphere (E_{in}) on the climate has not drawn much attention, due to the big challenge associated with its quantitative estimation. Based on a new E_{in} index estimated by three-dimensional magnetohydrodynamic simulations from a previous study, this study reveals that E_{in} exhibits both quasi-decadal variability (periodic 11-year) and interannual (2–4 years) variability, which has rarely before been detected by SSN and F10.7. A significant interannual relationship between the annual mean E_{in} and subsequent early-winter ENSO is further revealed. Following high E_{in} , the sea level pressure in the subsequent early winter shows significant positive anomalies from Asia southward to the Maritime Continent, and significant negative anomalies over the Southeast and Northeast Pacific, resembling the Southern Oscillation. Meanwhile, significant upper-level anomalous convergence and divergence winds appear over the western and eastern Pacific, which is configured with significant lower-level anomalous divergence and convergence, indicating a weakening of the Walker circulation. Consequently, notable surface easterly wind anomalies prevail over the eastern tropical Pacific, leading to El Niño-like sea surface temperature anomalies. It is suggested that better describing the processes in the solar wind–magnetosphere–ionosphere coupled system is essential to understand the solar influence on climate change.

摘要

作为地球系统的主要能量来源，进入地磁系统的太阳风能量通量 (E_{in}) 一直难以估算。因此， E_{in} 对气候的影响也没有得到广泛的研究。基于三维磁流体动力模拟估算的 E_{in} ，本文指出，太阳风能量通量不仅存在准11年周期的年代际变率，同时还存在2–4年周期的年际变率。与以往主要关注太阳活动在年代际尺度上的气候效应的研究不同，本文揭示出太阳风能量通量与次年 ENSO 年际变率存在显著的联系。

ARTICLE HISTORY

Received 13 November 2017
Revised 20 December 2017
Accepted 16 January 2018

KEYWORDS

Solar wind energy flux; ENSO; Walker circulation

关键词

太阳风能量通量; ENSO; Walker 环流

1. Introduction

It is well recognized that variations in solar irradiance, especially on quasi-decadal time scales, exert substantial effects on tropospheric climate (Christoforou and Hameed 1997; Gray et al. 2010; Herschel 1801; Liu and Lu 2010). Strong connections between the 11-year solar cycle (e.g. solar radio flux at 10.7 cm (F10.7) or sunspot number (SSN)) and climatic variability in the troposphere–lower stratosphere have been well documented (Ineson et al. 2011; Labitzke and Van Loon 1988, 1997; Loon and Labitzke 1988). For instance, both observational

and modelling results have documented the changes in regional and global pressure systems associated with the 11-year solar cycle, including the eastward (southward) migration of the Aleutian low (Hawaiian high) during minimum sunspots years (Christoforou and Hameed 1997), apparent positive pressure anomalies over the Gulf of Alaska in November–January of peak sunspots years (van Loon and Meehl 2008; Loon and Meehl 2014), and positive phases of the North Atlantic Oscillation in winters of maximum solar cycles (Kodera 2003; Thiéblemont et al. 2015).

CONTACT HE Sheng-Ping  Shengping.He@uib.no

© 2018 The Author(s). Published by Informa UK Limited, trading as Taylor & Francis Group.
This is an Open Access article distributed under the terms of the Creative Commons Attribution License (<http://creativecommons.org/licenses/by/4.0/>), which permits unrestricted use, distribution, and reproduction in any medium, provided the original work is properly cited.

Over the Pacific, one of the most dramatic features of sea level pressure (SLP) is the Southern Oscillation (SO) (Rasmusson and Carpenter 1982), together with El Niño/La Niña events, collectively known as El Niño–Southern Oscillation (ENSO) (Zebiak and Cane 1987). Previous studies have reported that ENSO is related to the internal cycle of feedback within the tropical Pacific ocean–atmosphere climatic systems (Chen, Chen, and Yu 2017; Chen et al. 2016; Chen and Zhou 2012; Graham and White 1988; McCreary Jr 1983; Nuzhdina 2002). Many recent studies have revealed that the extratropical forcing associated with large-scale atmospheric circulation plays very important roles in the formation of ENSO (Chen et al. 2013, 2015; Chen, Yu, and Chen 2014, 2015). Controversially, it has also been claimed that external forcing such as volcanic aerosols (Emile-Geay et al. 2008; Handler 1984) and Pacific bottom seismic events (Walker 1995) can explain the variability of ENSO. Additionally, the contribution of the 11-year solar cycle to the interdecadal variability of ENSO has been widely discussed (Kirov and Georgieva 2002; Marchitto et al. 2010; Troshichev et al. 2005). As the solar cycle cannot directly reflect the total energy contributing to Earth's atmosphere and is dominated by quasi-decadal variability (Ammann et al. 2007; Scafetta and West 2006), the interannual relationship between ENSO and solar activity, as well as the related mechanisms, is far from clear.

Although the total solar energy penetrating Earth's atmosphere is considerably smaller than the total solar irradiance, the interannual variability of the energy input from the solar wind is much larger (Troshichev et al. 2005). Therefore, it is very interesting to examine the interannual relationship between the total energy input from the solar wind into Earth's magnetosphere (E_{in}) and ENSO, which has rarely been discussed before because of the big challenge in quantitatively estimating E_{in} (Akasofu 1981; Newell et al. 2008). Based on a totally new E_{in} index, which is quantitatively estimated via three-dimensional magnetohydrodynamics (Wang et al. 2014), we reveal a statistically significant interannual relationship between the annual mean E_{in} and the subsequent early-winter ENSO.

2. Data and methods

2.1. Energy input from the solar wind into Earth's magnetosphere

A three-dimensional magnetohydrodynamic simulation is used to quantitatively estimate E_{in} (units: W), which is defined as follows (Wang et al. 2014):

$$E_{in} = 3.78 \times 10^7 n_{sw}^{0.24} V_{sw}^{1.47} B_T^{0.86} \left[\sin^{2.70} \left(\frac{\theta}{2} \right) + 0.25 \right]$$

Here, n_{sw} and V_{sw} are the solar wind number density (units: cm^{-3}) and solar wind velocity (units: km s^{-1}), respectively;

B_T is the transverse magnetic field magnitude (units: nT), and θ is the interplanetary magnetic field clock angle. Solar wind data is obtained from NASA OMNIweb (<http://omniweb.gsfc.nasa.gov/>). It has been suggested that E_{in} performs better than the empirical parameter used by Perreault and Akasofu (1978) in quantitatively estimating the energy input on the global scale (Wang et al. 2014).

2.2. Spatial data and other indices

Monthly mean atmospheric circulation data are obtained from the National Centers for Environmental Prediction–National Center for Atmospheric Research (NCEP/NCAR) reanalysis (Kalnay et al. 1996), with a horizontal resolution of $2.5^\circ \times 2.5^\circ$. To support the results derived from the NCEP/NCAR reanalysis, observational gridded monthly SLP data from the Met Office Hadley Center (HadISLP2r) are employed (Allan and Ansell 2006), with a horizontal resolution of $5^\circ \times 5^\circ$. The sea surface temperature (SST) data is also from the Met Office Hadley Centre (Rayner et al. 2003), with a horizontal resolution of $1^\circ \times 1^\circ$.

Given that the atmosphere plays an important role in transferring the solar signal to the ocean (Thiéblemont et al. 2015), we first use SO indices to investigate the relationship between E_{in} and ENSO. Three SO indices are calculated from the monthly SLP anomaly (SLPA) for the period January 1964 to December 2013, based on the method proposed by Schwing, Murphree, and Green (2002). The Northern Oscillation Index (NOI), which is roughly the North Pacific equivalent of the SO index, is defined as the difference in the SLPA between the climatological mean position of the center of the North Pacific high (35°N , 130°W) and Darwin (10°S , 130°E). One SO index (SIO1) is defined as the difference in the SLPA between the climatological mean position of the center of the South Pacific high (30°S , 95°W) and Darwin (10°S , 130°E), and the other (SIO2) is defined as the difference in the SLPA between Tahiti (18°S , 150°W) and Darwin (10°S , 130°E). SSN and F10.7 indices are obtained from National Centers for Environmental Information of the NOAA (<https://www.ngdc.noaa.gov/stp/solar/solar-indices.html>). All correlation and regression analyses are based on the detrended datasets.

3. Results

3.1. Different variability of E_{in} from SSN and F10.7

Considering that many previous studies have addressed the connection between SSN or F10.7 and climate (Huo and Xiao 2016; Nuzhdina 2002; Troshichev et al. 2005; Xiao and Li 2016; Xiao et al. 2017), we first discuss the difference between the solar wind energy and SSN/F10.7. Figure 1(a)–(c) display the normalized time series of

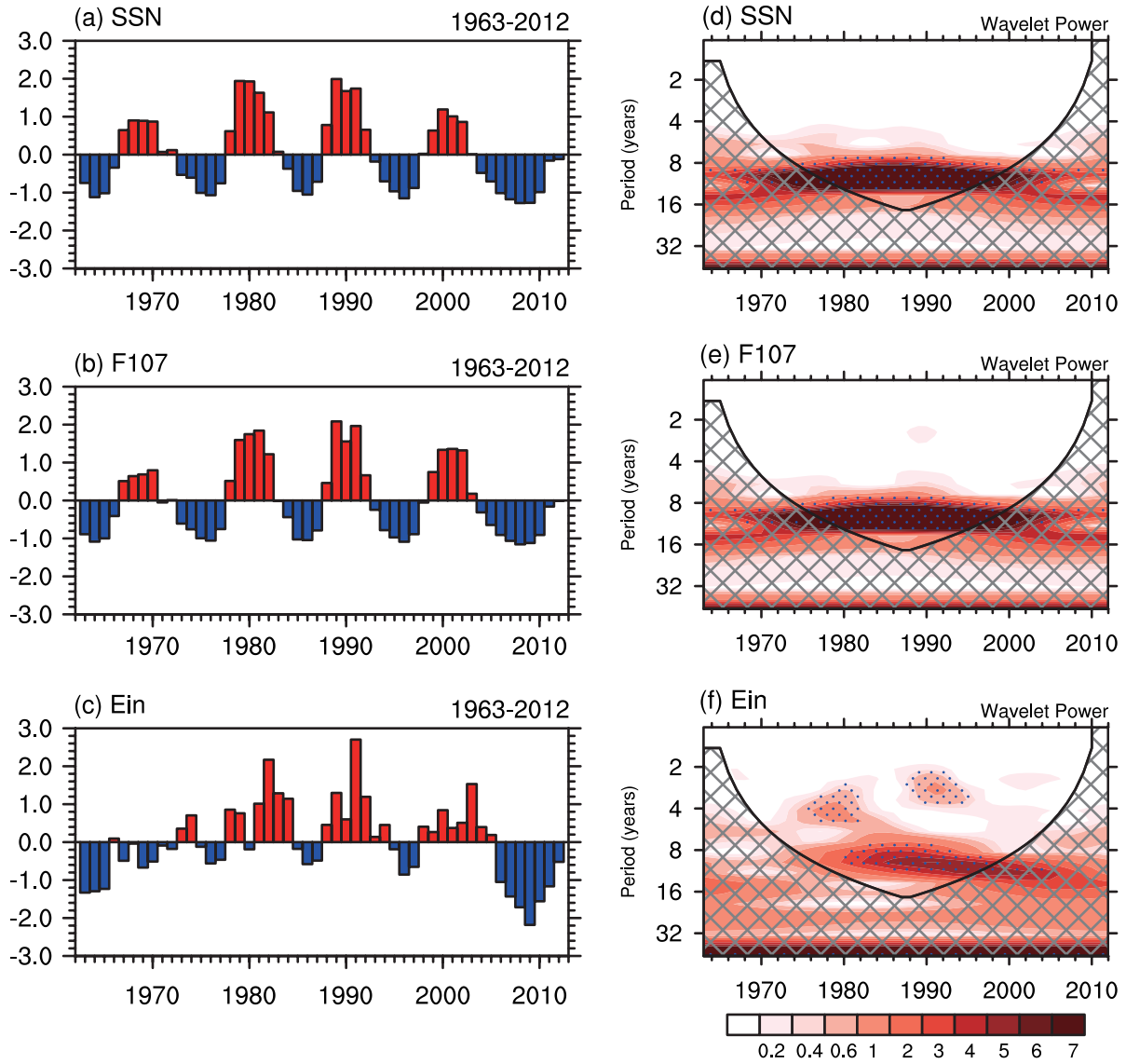


Figure 1. Normalized time series of annual-mean (a) SSN, (b) F10.7, and (c) E_{in} during 1963–2012. Morlet wavelet analysis for the standardized time series of annual-mean (d) SSN, (e) F10.7, and (f) E_{in} . Notes: The dotted regions are statistically significant at the 95% confidence level for a red-noise process. Cross-hatched regions on either end indicate the ‘cone of influence’, where edge effects become important.

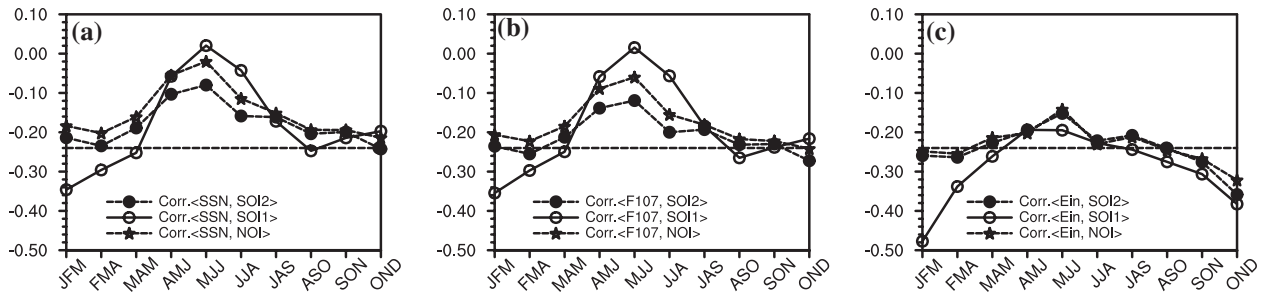


Figure 2. Evolution of the lagged (SO lags solar activity) correlation coefficients between the annual-mean (a) SSN, (b) F10.7, and (c) E_{in} during 1963–2012 and the seasonal-mean SO indices during 1964–2013.

Note: The dashed lines indicate statistically significant correlation coefficients at the 90% confidence level.

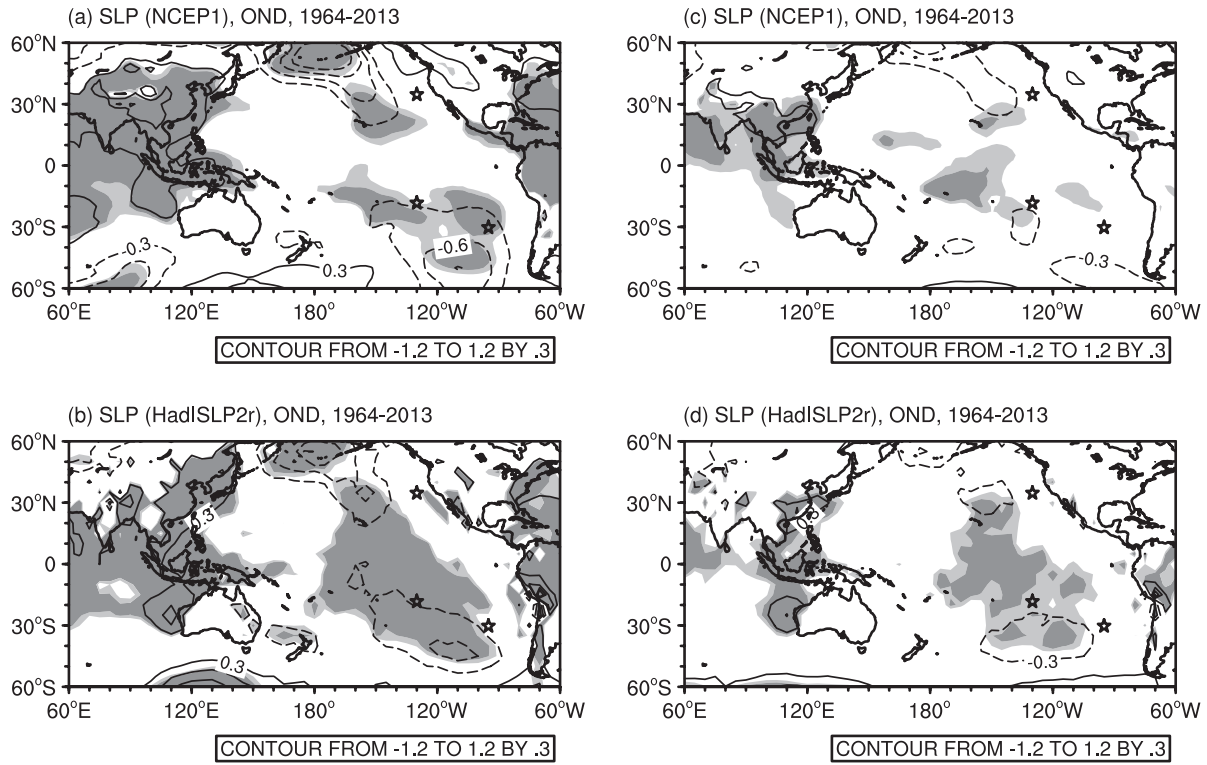


Figure 3. (a, b) Regression maps of NCEP1/Hadley SLP (contours; units: hPa) in early winter 1964–2013 upon the E_{in} during 1963–2012. Light and dark shading indicates statistical significance at the 90% and 95% confidence level, respectively. (c, d) As in (a, b) but regressed upon SSN.

Notes: The pentagrams indicate the position of the centers of SLP in the North Pacific (35°N, 130°W), Darwin and Australia (10°S, 130°E), the South Pacific (30°S, 95°W), and Tahiti (18°S, 150°E); the same in subsequent figures.

annual-mean SSN, F10.7 and E_{in} during 1963–2012. It is apparent that SSN and F10.7 are dominated by low-frequency variability, with alternate positive and negative phases (Figure 1(a) and (b)). Morlet wavelet analysis indicates that SSN and F10.7 show clear low-frequency oscillation, with a period of about 11 years (Figure 1(d) and (e)). Moreover, the wavelet power of SSN and F10.7 with periods below 8 years is not statistically significant. In contrast, the periodicity of E_{in} is not as stable as that of SSN and F10.7. It displays both interannual and decadal variability (Figure 1(c)), which is more apparent by inspecting Figure 1(f). The indication is that E_{in} is dominated by variability with 2–4-year and 8–11-year periodicity (Figure 1(f)). These results are also supported by spectral analysis (data not shown). Additionally, compared with the high correlation coefficient of 0.988 between SSN and F10.7, the correlation coefficients of 0.637/0.647 between E_{in} and SSN/F10.7 imply a notable difference between E_{in} and SSN/F10.7.

3.2. Linkages between atmospheric circulation and E_{in}

To confirm a robust linkage between ENSO and E_{in} , we adopt three different SO indices (NOI, SIO1, and SIO2, as

outlined in Section 2.2). The temporal evolution of the lagged correlations between the annual-mean E_{in} and the seasonal-mean SO indices indicates that significant correlations start to emerge in the following autumn, with the strongest correlation in the following early winter (October to December) (Figure 2(c)). In contrast, such a statistically significant interannual relationship is not observed between the 11-year solar cycle (i.e. SSN or F10.7) and the SO indices (Figures 2(a) and (b)). This implies that the annual accumulation of solar energy potentially contributes to the interannual variability of the SO in the following early winter.

To give more detail on the different influences between E_{in} and SSN/F10.7, we present in Figure 3 the regression of early-winter SLP upon the preceding annual E_{in} and SSN. At lag(+1 yr) of high total solar wind energy penetrating Earth's magnetosphere, the early-winter SLP shows statistically significant anomalies over Asia, the eastern Indian Ocean, the western Pacific, the North and South Pacific, and the United States (Figure 3(a)). A statistically significant high-pressure anomaly (0.3–1.4 hPa) extends from Asia southward to the Maritime Continent (between 40°S and 40°N), and a significant low-pressure anomaly (–1.2 to –0.2 hPa) is located in the subtropical North (20°–60°N)

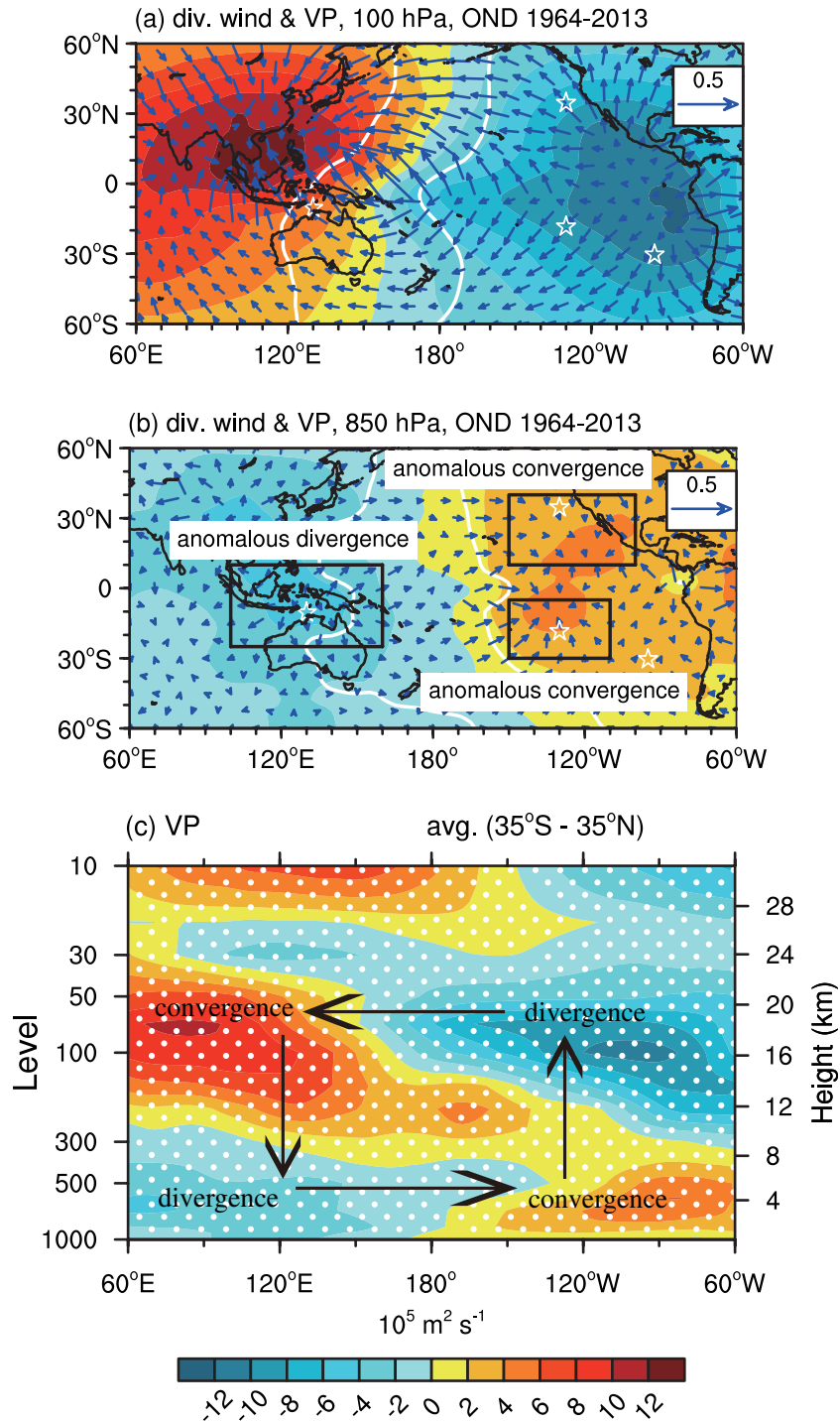


Figure 4. Regression maps of the divergence component of the wind (div; vectors; units: m s^{-1}) and velocity potential (VP; shading; units: $10^5 \text{ m}^2 \text{ s}^{-1}$) at (a) 100 hPa and (b) 850 Pa in early winter 1964–2013 upon the E_{in} during 1963–2012. (c) As in (a) but for a vertical–longitude cross section of VP averaged over (35°S–35°N).

Notes: Values enclosed by contours in (a) and (b) and stippling in (c) indicate statistically significant VP anomalies at the 90% confidence level. The black arrows in (c) are a schematic representation of the anomalous Walker circulation.

and South (60°–20°S) Pacific. The spatial distribution derived from HadSLP2r is similar to that from the NCEP/NCAR reanalysis (Figure 3(b)), indicating the robustness of the results. Such an anomalous pressure pattern, resembling the SO (Rasmusson and Carpenter 1982; Schwing,

Murphree, and Green 2002), has rarely been detected before by crude composite differences between maximum and minimum solar phases. As illustrated by Figure 3(c) and (d), the SLPAs related to SSN are less significant and smaller in magnitude than those related to E_{in} .

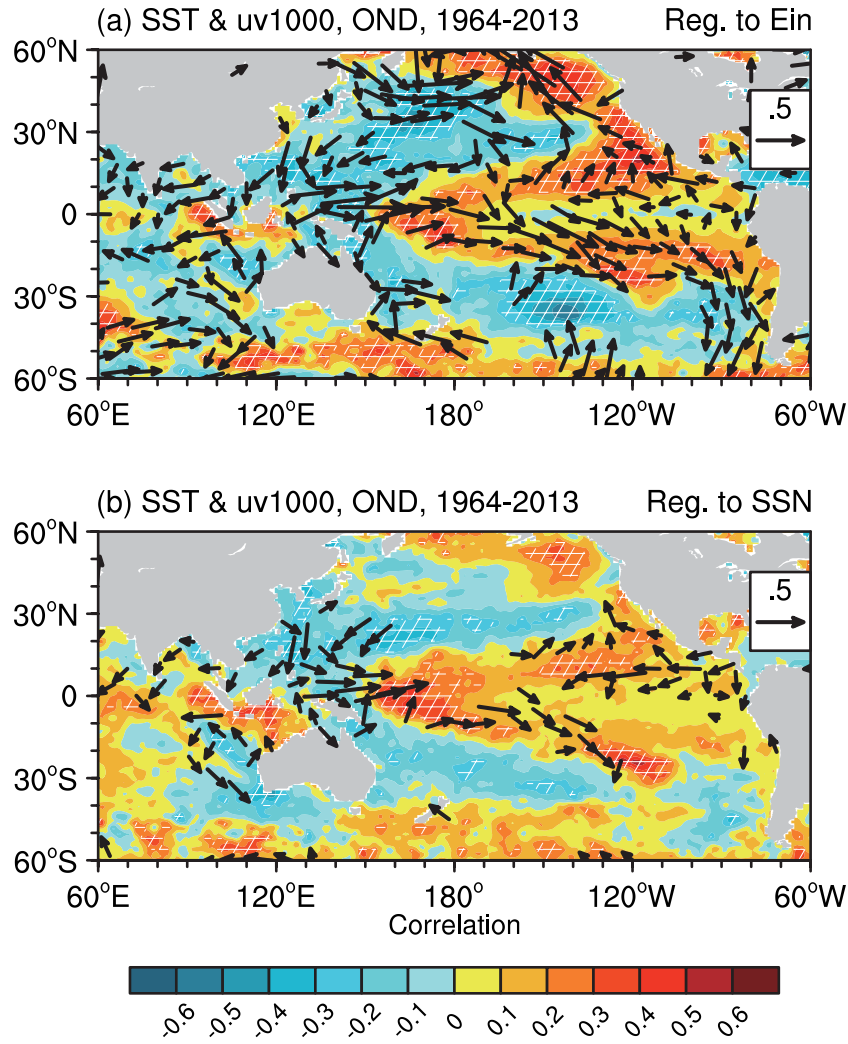


Figure 5. Correlation/regression of SST (shading)/1000-hPa wind (vectors; units: m s^{-1}) in early winter 1964–2013 upon the (a) E_{in} / (b) SSN during 1963–2012. Cross-hatched areas indicate statistically significant values at the 90% confidence level. Note: Winds are only displayed if either component of the wind anomalies is statistically significant at the 90% confidence level.

3.3. Anomalous atmospheric dynamical processes of ENSO associated with E_{in}

Linear regression of early-winter velocity potential at lag(+1 yr) onto E_{in} shows a zonally oriented dipole pattern with opposite sign at the near surface (850 hPa ≈ 1.4 km) and upper level (100 hPa ≈ 16 km) (Figure 4(a) and (b)). At 850 hPa, a statistically significant anomalous divergence center (approximately $-4.0 \times 10^5 \text{ m}^2 \text{ s}^{-1}$) is strictly confined to Darwin Island, accompanied by two statistically significant positive centers located around Tahiti Island and the Northeast Pacific (35°N, 130°W) (Figure 4(b), shading). Similar results but with opposite sign are apparent in the upper troposphere. Note that the velocity potential anomaly in the upper troposphere is stronger, with a magnitude as high as $1.4 \times 10^6 \text{ m}^2 \text{ s}^{-1}$ (Figure 4(a), shading). Additionally, apparent significant anomalous divergence and convergence winds appear where negative and

positive velocity potential anomaly centers are located (Figure 4(a) and (b), vectors). It should be noted that the significant anomalous divergence/convergence winds are observed in the locations used to identify the SO indices (Figure 4(b), blue boxes), confirming the significant influence of E_{in} on the formation of the SO. This is further supported by the cross section (averaged between 35°S and 35°N) of velocity potential, which indicates that the anomalies west of the date line are opposite to those in the east, and the sign also reverses at ~ 400 hPa or ~ 7 km (Figure 4(c)). The configuration of anomalous divergence/convergence indicates a pronounced weakening of the Pacific Hadley–Walker circulation (Bjerknes 1966), which is an important dynamical contributor to the formation of the SO (Schwing, Murphree, and Green 2002). As a result, corresponding to an increasing of the total energy input from the solar wind penetrating Earth’s magnetosphere,

the atmospheric circulation in the subsequent early winter is characterized by anomalous surface westerly winds ($\sim 0.5 \text{ m s}^{-1}$) across the central and eastern tropical Pacific (Figure 5(f), vectors). Meanwhile, anomalous rising motion over the eastern Pacific, a returning flow ($\sim 0.5 \text{ m s}^{-1}$) from east to west at the upper level of the troposphere, and anomalous sinking motion over the western Pacific are observed (data not shown). The change in atmospheric circulation, especially the surface anomalous westerly ($\sim 0.5 \text{ m s}^{-1}$) in the central and eastern tropical Pacific, leads to an El Niño-like SST anomaly pattern (Figure 5(a), shading) (Li 1990). In contrast, the early-winter surface wind related to the preceding SSN barely shows any significant anomalies (Figure 5(b), vectors). Correspondingly, the correlation between SSN and SST is much weaker (Figure 5(b), shading). We speculate that the solar ultraviolet irradiance effect associated with E_{in} and the atmospheric internal variability (i.e. Brewer–Dobson circulation) might be the main mechanism of such a significant lag correlation.

4. Discussion

Recent analyses of the relationship between solar activity and atmospheric processes conducted by comparing two multi-decadal ocean–atmosphere chemistry–climate simulations with and without solar forcing variability revealed a significant response of the boreal winter atmosphere at lag(+1 yr) to the 11-year solar cycle (i.e. F10.7) (Thiéblemont et al. 2015). Although they found statistically significant SLPAs over the Atlantic–Arctic regions, the signals in other regions (e.g. the North Pacific) have not drawn much attention. As the 11-year solar cycle is dominated by quasi-decadal variability and cannot directly reflect the total energy contributed to Earth's atmosphere, the relationship between solar activity and the atmosphere at the interannual time scale remains unclear.

This study, based on a new index estimated by three-dimensional magneto hydrodynamic simulations (Wang et al. 2014), reveals a new statistically significant interannual relationship between the annual-mean solar wind energy penetrating Earth's magnetosphere and the subsequent early-winter ENSO. The annual accumulation of solar wind energy may explain more of the total interannual variance of ENSO compared to SSN/F10.7. Therefore, this study suggests that, even though it might be a big challenge, describing the processes of energy transmission, conversion and dissipation well in the solar wind–magnetosphere–ionosphere coupled system is essential to understand climate change and improve climate prediction.

Disclosure statement

No potential conflict of interest was reported by the authors.

Funding

This research was supported by the National Key R&D Program of China [grant number 2016YFA0600703], the National Natural Science Foundation of China [grant numbers 41421004, 41505073, and 41605059], and the Young Talent Support Plan launched by the China Association for Science and Technology [grant number 2016QNR001].

References

- Akasofu, S.-I. 1981. "Energy Coupling between the Solar Wind and the Magnetosphere." *Space Science Reviews* 28: 121–190.
- Allan, R., and T. Ansell. 2006. "A New Globally Complete Monthly Historical Gridded Mean Sea Level Pressure Dataset (HadSLP2): 1850–2004." *Journal of Climate* 19: 5816–5842.
- Ammann, C. M., F. Joos, D. S. Schimel, B. L. Otto-Bliesner, and R. A. Tomas. 2007. "Solar Influence on Climate during the past Millennium: Results from Transient Simulations with the NCAR Climate System Model." *Proceedings of the National Academy of Sciences of the United States of America* 104: 3713–3718.
- Bjerknes, J. 1966. "A Possible Response of the Atmospheric Hadley Circulation to Equatorial Anomalies of Ocean Temperature." *Tellus* 18: 820–829.
- Chen, S., W. Chen, and B. Yu. 2017. "The Influence of Boreal Spring Arctic Oscillation on the Subsequent Winter ENSO in CMIP5 Models." *Climate Dynamics* 48: 2949–2965.
- Chen, S., W. Chen, B. Yu, and H. F. Graf. 2013. "Modulation of the Seasonal Footprinting Mechanism by the Boreal Spring Arctic Oscillation." *Geophysical Research Letters* 40: 6384–6389.
- Chen, S., R. Wu, W. Chen, and B. Yu. 2015. "Influence of the November Arctic Oscillation on the Subsequent Tropical Pacific Sea Surface Temperature." *International Journal of Climatology* 35: 4307–4317.
- Chen, S., R. Wu, W. Chen, B. Yu, and X. Cao. 2016. "Genesis of Westerly Wind Bursts over the Equatorial Western Pacific during the Onset of the Strong 2015–2016 El Niño." *Atmospheric Science Letters* 17: 384–391.
- Chen, S., B. Yu, and W. Chen. 2014. "An Analysis on the Physical Process of the Influence of AO on ENSO." *Climate Dynamics* 42: 973–989.
- Chen, S., B. Yu, and W. Chen. 2015. "An Interdecadal Change in the Influence of the Spring Arctic Oscillation on the Subsequent ENSO around the Early 1970s." *Climate Dynamics* 44: 1109–1126.
- Chen, W., and Q. Zhou. 2012. "Modulation of the Arctic Oscillation and the East Asian Winter Climate Relationships by the 11-Year Solar Cycle." *Advances in Atmospheric Sciences* 29: 217–226.
- Christoforou, P., and S. Hameed. 1997. "Solar Cycle and the Pacific 'Centers of Action.'" *Geophysical Research Letters* 24: 293–296.
- Emile-Geay, J., R. Seager, M. A. Cane, E. R. Cook, and G. H. Haug. 2008. "Volcanoes and ENSO Over the Past Millennium." *Journal of Climate* 21: 3134–3148.
- Graham, N. E., and W. B. White. 1988. "The El Niño Cycle: A Natural Oscillator of the Pacific Ocean–Atmosphere System." *Science* 240: 1293–1302.
- Gray, L. J., J. Beer, M. Geller, J. D. Haigh, M. Lockwood, K. Matthes, U. Cubasch, et al. 2010. "Solar Influences on Climate." *Reviews of Geophysics* 48 (4): RG4001. doi:10.1029/2009RG000282.

- Handler, P. 1984. "Possible Association of Stratospheric Aerosols and El Niño Type Events." *Geophysical Research Letters* 11: 1121–1124.
- Herschel, W. 1801. "Observations Tending to Investigate the Nature of the Sun, in Order to Find the Causes or Symptoms of Its Variable Emission of Light and Heat; with Remarks on the Use That May Possibly Be Drawn from Solar Observations." *Philosophical Transactions of the Royal Society of London* 91: 265–318.
- Huo, W.-J., and Z.-N. Xiao. 2016. "The Impact of Solar Activity on the 2015/16 El Niño Event." *Atmospheric and Oceanic Science Letters* 9: 428–435.
- Ineson, S., A. A. Scaife, J. R. Knight, J. C. Manners, N. J. Dunstone, L. J. Gray, and J. D. Haigh. 2011. "Solar Forcing of Winter Climate Variability in the Northern Hemisphere." *Nature Geoscience* 4: 753–757.
- Labitzke, K., and H. Van Loon. 1997. "The Signal of the 11-Year Sunspot Cycle in the Upper Troposphere-Lower Stratosphere." *Space Science Reviews* 80: 393–410.
- Kalnay, E., M. Kanamitsu, R. Kistler, W. Collins, D. Deaven, L. Gandin, M. Iredell, et al. 1996. "The NCEP/NCAR 40-Year Reanalysis Project." *Bulletin of the American Meteorological Society* 77: 437–471.
- Kirov, B., and K. Georgieva. 2002. "Long-Term Variations and Interrelations of ENSO, NAO and Solar Activity." *Physics and Chemistry of the Earth, Parts a/B/C* 27: 441–448.
- Kodera, K. 2003. "Solar Influence on the Spatial Structure of the NAO during the Winter 1900–1999." *Geophysical Research Letters* 30 (4): 1175. doi:10.1029/2002GL016584.
- Labitzke, K., and H. Van Loon. 1988. "Associations between the 11-Year Solar Cycle, the QBO and the Atmosphere. Part I: The Troposphere and Stratosphere in the Northern Hemisphere in Winter." *Journal of Atmospheric and Terrestrial Physics* 50: 197–206.
- Li, C. Y. 1990. "Interaction between Anomalous Winter Monsoon in East Asia and El Niño Events." *Advances in Atmospheric Sciences* 7: 36–46.
- Liu, Y., and C. H. Lu. 2010. "The Influence of the 11-Year Sunspot Cycle on the Atmospheric Circulation during Winter." *Chinese Journal of Geophysics* 53: 354–364.
- Loon, H. V., and K. Labitzke. 1988. "Association between the 11-Year Solar Cycle, the QBO, and the Atmosphere. Part II: Surface and 700 Mb in the Northern Hemisphere in Winter." *Journal of Climate* 1: 905–920.
- van Loon, H., and G. A. Meehl. 2008. "The Response in the Pacific to the Sun's Decadal Peaks and Contrasts to Cold Events in the Southern Oscillation." *Journal of Atmospheric and Solar-Terrestrial Physics* 70: 1046–1055.
- Loon, H., and G. A. Meehl. 2014. "Interactions between Externally Forced Climate Signals from Sunspot Peaks and the Internally Generated Pacific Decadal and North Atlantic Oscillations." *Geophysical Research Letters* 41: 161–166.
- Marchitto, T. M., R. Muscheler, J. D. Ortiz, J. D. Carriquiry, and A. van Geen. 2010. "Dynamical Response of the Tropical Pacific Ocean to Solar Forcing during the Early Holocene." *Science* 330: 1378–1381.
- McCreary Jr, J. P. 1983. "A Model of Tropical Ocean-Atmosphere Interaction." *Monthly Weather Review* 111: 370–387.
- Newell, P. T., T. Sotirelis, K. Liou, and F. Rich. 2008. "Pairs of Solar Wind-Magnetosphere Coupling Functions: Combining a Merging Term with a Viscous Term Works Best." *Journal of Geophysical Research* 113: A04218. doi:10.1029/2007JA012825.
- Nuzhdina, M. 2002. "Connection between ENSO Phenomena and Solar and Geomagnetic Activity." *Natural Hazards and Earth System Science* 2: 83–89.
- Perreault, P., and S. I. Akasofu. 1978. "A Study of Geomagnetic Storms." *Geophysical Journal International* 54 (3): 547–573.
- Rasmusson, E. M., and T. H. Carpenter. 1982. "Variations in Tropical Sea Surface Temperature and Surface Wind Fields Associated with the Southern Oscillation/El Niño." *Monthly Weather Review* 110: 354–384.
- Rayner, N. A., D. E. Parker, E. B. Horton, C. K. Folland, L. V. Alexander, D. P. Rowell, E. C. Kent, and A. Kaplan. 2003. "Global Analyses of Sea Surface Temperature, Sea Ice, and Night Marine Air Temperature since the Late Nineteenth Century." *Journal of Geophysical Research Atmospheres* 108: 1063–1082.
- Scafetta, N., and B. West. 2006. "Phenomenological Solar Contribution to the 1900–2000 Global Surface Warming." *Geophysical Research Letters* 33: L05708. doi:10.1029/2005GL025539.
- Schwing, F., T. Murphree, and P. Green. 2002. "The Northern Oscillation Index (NOI): A New Climate Index for the Northeast Pacific." *Progress in Oceanography* 53: 115–139.
- Thiéblemont, R., K. Matthes, N.-E. Omrani, K. Kodera, and F. Hansen. 2015. "Solar Forcing Synchronizes Decadal North Atlantic Climate Variability." *Nature Communications* 6: 8268.
- Troshichev, O., L. Egorova, A. Janzhura, and V. Vovk. 2005. "Influence of the Disturbed Solar Wind on Atmospheric Processes in Antarctica and El-Niño Southern Oscillation (ENSO)." *Memorie Societa Astronomica Italiana* 76 (4): 890.
- Walker, D. A. 1995. "More Evidence Indicates Link between El Niños and Seismicity." *EOS, Transactions American Geophysical Union* 76: 33–36.
- Wang, C., J. Han, H. Li, Z. Peng, and J. Richardson. 2014. "Solar Wind-Magnetosphere Energy Coupling Function Fitting: Results from a Global MHD Simulation." *Journal of Geophysical Research: Space Physics* 119: 6199–6212.
- Xiao, Z., and D. Li. 2016. "Solar Wind: A Possible Factor Driving the Interannual Sea Surface Temperature Tripolar Mode over North Atlantic." *Journal of Meteorological Research* 30: 312–327.
- Xiao, Z.-N., D.-L. Li, L.-M. Zhou, L. Zhao, and W.-J. Huo. 2017. "Interdisciplinary Studies of Solar Activity and Climate Change." *Atmospheric and Oceanic Science Letters* 1–4.
- Zebiak, S. E., and M. A. Cane. 1987. "A Model El Niño-Southern Oscillation." *Monthly Weather Review* 115: 2262–2278.